Article

Hopf Bifurcation of the Oregonator Oscillator with Distributed Delay

Yu Wang [1,*] and Luca Guerrini [2]

[1] School of Mathematics, Southeast University, Nanjing 210096, China
[2] Department of Management, Polytechnic University of Marche, 60121 Ancona, Italy
[*] Correspondence: 230218180@seu.edu.cn

Received: 2 June 2024; Revised: 10 July 2024; Accepted: 30 July 2024; Published: 19 August 2024

Abstract: This paper investigates the bifurcation problem of the Oregonator oscillator with distributed time delay, and two cases are considered, namely weak and strong kernels. First, theoretical approaches are provided to analyze the stability properties of the equilibrium in these systems using the chain trick method. Near the positive equilibrium point, the Routh-Hurwitz criteria are employed to establish precise conditions for stability and Hopf bifurcation and determine the bifurcation direction. Additionally, this paper explores the implications of infinite memory within a distributed delay to gain insights into the dynamic behavior. Moreover, extensive numerical simulations are conducted to support our theoretical analysis. The main simulations illustrate the bifurcation waveform and phase diagrams and reveal complex dynamic behavior, including stable and unstable oscillations.

Keywords: distributed delay; oregonator oscillator; stability; hopf bifurcation

1. Introduction

Time delay is a crucial factor for understanding the intricate dynamics of various chemical reaction systems. In this domain, an interesting subset of delayed systems can exhibit oscillatory behavior, showing that the concentrations of essential reactants will undergo stable cyclic changes [1–10].

The investigation of oscillatory chemical reactions can be traced back to 1921, and Bray's experimental achievement of a liquid oscillatory reaction marked an important milestone in the field [11]. Drawing on Bray's work, in 1964, Zhabotinsky's report of additional oscillatory reactions with similar characteristics further deepened the understanding of these dynamic phenomena [12]. This led to more interest and investigation into the underlying mechanisms governing the oscillatory behavior of chemical systems, and some studies were conducted with the introduction of the Oregonator model. These comprehensive studies not only provided valuable insights into the intricacies of oscillatory chemical reactions but also made significant contributions to the evolving understanding of the Oregonator model itself [13–17].

Recently, in *Hopf-zero bifurcation of Oregonator oscillator with delay*, Cai et al. [16] investigated the Hopf bifurcation phenomenon in the Oregonator oscillator. The model was extended by incorporating discrete delays, with a consideration of the inherent time lags in reactions and transport processes. The model is characterized by a system of delay differential equations, as shown below

$$\begin{cases} \dot{x} &= \dfrac{x(1-x)}{\varepsilon} - \dfrac{h_1 z}{\varepsilon}\dfrac{x-q}{x+q}, \\ \dot{z} &= x - z + kz(t-\tau), \end{cases} \tag{1}$$

where $x = [\mathrm{HBrO_2}]$, z =Ce(IV), $\varepsilon = 4 \cdot 10^{-2}$, $q = 8 \cdot 10^{-4}$, $k < 1$ and $h_1 \in (0, 1)$ is an adjustable parameter. The system described by Equation (1) has a distinct positive steady state, which can be calculated as

$$x_+ = \frac{1 - \dfrac{h_1}{1-k} - q + \sqrt{\left(1 - \dfrac{h_1}{1-k} - q\right)^2 + 4q\left(1 + \dfrac{h_1}{1-k}\right)}}{2}, \qquad z_+ = \frac{x_+}{1-k}.$$

The inclusion of delays reveals a rich and complex dynamic range and focuses on analyzing the stability and bifurcation properties of this delayed system, especially how delays lead to phenomena such as amplitude death and mixed-mode oscillations.

Recent studies on Hopf bifurcation in delay-coupled systems have emphasized the complex dynamical be-

haviors induced by discrete time delays. These studies demonstrate how delays can result in bifurcations, affect synchronization and stability, and lead to the emergence of hidden attractors [18–20]. Despite these advancements, it is still necessary to investigate distributed time delays, which better represent where interactions occur over long periods of time. However, the Hopf-zero bifurcation of the Oregonator oscillator with distributed time delay has not been studied, which has far-reaching significance to research.

Research has indicated that distributed time delays have a significant impact on the dynamic properties of complex systems and have been used in widespread practical applications [2, 21–23]. In chemical reactions, delays arising from diffusion processes play a crucial role in shaping the overall dynamics. Grasping the effects of these delays is the key to developing more accurate models that capture the intricacies of real systems [4, 24–27]. Distributed delay systems generally exhibit richer dynamics than transient systems [10, 28, 29]. Motivated by this observation, this paper will address this challenging issue.

Our study focuses on the stability and Hopf bifurcation of the distributed delay Oregonator oscillator. Stability analysis provides insight into the long-term behavior of the system. The Hopf bifurcation points are important for understanding and controlling the oscillatory behavior of the system. The rest of this paper is structured as follows: the mathematical model of the Oregonator oscillator with distributed time delays is introduced in Section 2. Section 3 investigates the stability conditions for the model with the weak kernel. The stability criteria and Hopf bifurcation analysis for the model characterized by the strong kernel are presented in Section 4. The applicability of the proposed theoretical work is validated by numerical examples in Section 5. Finally, Section 6 summarizes the results and discusses the potential topic for future research.

2. The Model

In this study, an extension of the model (1) is introduced, which enhances its generality by replacing discrete delays with distributed delays, as shown below

$$\begin{cases} \dot{x} &= \dfrac{x(1-x)}{\varepsilon} - \dfrac{h_1 z}{\varepsilon}\dfrac{x-q}{x+q}, \\ \dot{z} &= x - z + k\displaystyle\int_{-\infty}^{t} z(s)g(t-s)ds, \end{cases} \tag{2}$$

where $g(\cdot)$ is a gamma distribution, i.e.,

$$g(\xi) = \frac{\alpha^m \xi^{m-1} e^{-\alpha\xi}}{(m-1)!},$$

where m plays an important role in shaping the weighting function with an average delay of $T = m/\alpha$, which is a positive integer. As T approaches 0, the distribution function tends to be the Dirac distribution, allowing for a return to the discrete time delay case. Therefore, discrete delays can be considered as a special case or a limiting scenario of distributed delays. Let α be the bifurcation parameter, to investigate the stability and Hopf bifurcation of the system described in Equation (2), this paper employs the linear chain approach, as outlined in [30]. This method allows for transforming the distributed delay differential equations given by (2) into ordinary differential equations. Following Cushing's idea [31], two commonly encountered kernels in the literature are considered in this study: the weak kernel, defined as $g(\xi) = \alpha e^{-\alpha\xi}$, and the strong kernel, defined as $g(\xi) = \alpha^2 \xi e^{-\alpha\xi}$.

3. Weak Kernel Case

The new variable u is defined as follows for the sake of convenience

$$u = \int_{-\infty}^{t} z(s)\alpha e^{-\alpha(t-s)}ds.$$

By employing the linear chain technique, system (2) is transformed into the equivalent system shown below

$$\begin{cases} \dot{x} &= \dfrac{x(1-x)}{\varepsilon} - \dfrac{h_1 z}{\varepsilon}\dfrac{x-q}{x+q}, \\ \dot{z} &= x - z + ku, \\ \dot{u} &= \alpha(z-u). \end{cases} \tag{3}$$

Now, the stability and Hopf bifurcation of the system (3) are analyzed by examining the eigenvalues of the linearized systems near its equilibrium point (x_+, z_+, u_+), where $u_+ = z_+$. The characteristic equation is expressed as follows

$$\begin{vmatrix} a_1 - \lambda & a_2 & 0 \\ 1 & -1 - \lambda & k \\ 0 & \alpha & -\alpha - \lambda \end{vmatrix} = 0, \tag{4}$$

where λ denotes a characteristic root and

$$a_1 = \frac{1 - 2x_+}{\varepsilon} - \frac{2h_1 q z_+}{\varepsilon (x_+ + q)^2}, \qquad a_2 = -\frac{h_1 (x_+ - q)}{\varepsilon (x_+ + q)}.$$

A direct calculation indicates that (4) results in

$$\lambda^3 + c_1(\alpha)\lambda^2 + c_2(\alpha)\lambda + c_3(\alpha) = 0, \tag{5}$$

where

$$c_1(\alpha) = -b_1 + \alpha, \quad c_2(\alpha) = -b_2 - \alpha (b_1 + k), \qquad c_3(\alpha) = -\alpha (b_2 - k a_1),$$

with

$$b_1 = a_1 - 1, \qquad b_2 = a_1 + a_2.$$

3.1. Case $c_3(\alpha) = 0$

Then, Equation (5) becomes

$$P(\lambda, \alpha) = \lambda^3 + c_1(\alpha)\lambda^2 + c_2(\alpha)\lambda = 0. \tag{6}$$

Proposition 1.

(1) *If $c_2(\alpha) \neq 0$, then the characteristic Equation (6) has a simple zero root and a pair of purely imaginary roots $\pm i\omega_*$, where $\omega_* = \sqrt{c_2(\alpha_*)}$, if $c_1(\alpha_*) = 0$ and $c_2(\alpha_*) > 0$. The equilibrium point (x_+, z_+, u_+) of (3) is stable if and only if $c_1(\alpha) > 0$ and $c_2(\alpha) > 0$.*

(2) *If $c_2(\alpha) = 0$ and $c_1(\alpha) \neq 0$, then the characteristic Equation (6) has a double zero root and the root $\lambda = -c_1(\alpha)$. The equilibrium point (x_+, z_+, u_+) of (3) is stable if and only if $c_1(\alpha) > 0$.*

(3) *If $c_2(\alpha) = 0$ and $c_1(\alpha) = 0$, the characteristic Equation (6) has a triple zero root.*

Proof. Apparently, $\lambda = 0$ is a root of (6). The derivative with respect to λ in (6) gives

$$\frac{\partial P(\lambda, \alpha)}{\partial \lambda} = 3\lambda^2 + 2c_1(\alpha)\lambda + c_2(\alpha).$$

Thus, $\partial P(0, \alpha)/\partial \lambda = 0$ if and only if $c_2(\alpha) = 0$. Therefore, $\lambda = 0$ has multiplicity one when $c_2(\alpha) = 0$. Additionally, we have

$$\frac{\partial^2 P(\lambda, \alpha)}{\partial \lambda^2} = 6\lambda + 2c_1(\alpha), \qquad \frac{\partial^3 P(\lambda, \alpha)}{\partial \lambda^3} = 6,$$

which implies that $\partial^2 P(0, \alpha)/\partial \lambda^2 = 0$ if and only if $c_1(\alpha) = 0$, $\partial^3 P(0, \alpha)/\partial \lambda^3 = 6$. The first part of the statement holds.

Let $c_2(\alpha) \neq 0$ and $c_1(\alpha) \neq 0$. All the roots in (6), except for $\lambda = 0$, are governed by the quadratic equation

$$\lambda^2 + c_1(\alpha)\lambda + c_2(\alpha) = 0.$$

Applying the Routh-Hurwitz criteria, if all coefficients of this equation are positive, then all its roots have negative real parts.

Next, this paper investigates the conditions in which (6) has a pair of purely imaginary roots. If $\lambda = i\omega$, $\omega > 0$, is a root of (6), then rewriting the characteristic equation (6) by expressing its real and imaginary components separately yields $-\omega^2 + c_2(\alpha) = 0$ and $c_1(\alpha)\omega = 0$. Therefore, we have $c_1(\alpha) = 0$ and $\omega = \sqrt{c_2(\alpha)}$, with $c_2(\alpha) > 0$.

Let $c_2(\alpha) = 0$ and $c_1(\alpha) \neq 0$. Equation (6) becomes

$$\lambda^2 \left[\lambda + c_1(\alpha)\right] = 0,$$

yielding the root $\lambda = -c_1(\alpha)$. This completes the proof. □

Proposition 2. *The equilibrium point* (x_+, z_+, u_+) *of* (3) *has no stability switch* (*from unstable to stable*) *at* $\alpha = \alpha_* > 0$, *where* α_* *solves* $c_1(\alpha_*) = 0$ *and* $c_2(\alpha_*) > 0$.

Proof. Differentiating Equation (6) with respect to α leads to

$$Re\left(\frac{d\lambda}{d\alpha}\right)_{\lambda=i\omega_*} = Re\left[-\frac{c_1'(\alpha)\lambda + c_2'(\alpha)}{2\lambda + c_1(\alpha)}\right]_{\lambda=i\omega_*} = -\frac{2c_1'(\alpha_*)c_2(\alpha_*) + c_2'(\alpha_*)c_1(\alpha_*)}{4\omega_*^2 + c_1^2(\alpha_*)} = -\frac{1}{2} < 0,$$

where $c_2(\alpha_*) = \omega_*^2 > 0$, $c_1(\alpha_*) = 0$, i.e., $\alpha_* = -b_1 > 0$, $c_1'(\alpha_*) = 1$ and $c_2'(\alpha_*) = -b_1 - k$. The negative sign in the above inequality indicates that increasing the value of α leads to crossing of the imaginary axis from right to left. As a result, stability cannot be achieved at the critical value α_*. □

3.2. Case $c_3(\alpha) \neq 0$

Based on the Routh-Hurwitz criteria, the characteristic Equation (5) has three eigenvalues with negative real parts if and only if $c_1(\alpha) > 0, c_3(\alpha) > 0$ and $c_1(\alpha)c_2(\alpha) > c_3(\alpha)$. Particularly, one has $c_2(\alpha) > 0$. These inequalities lead to

$$\alpha > b_1, \qquad b_2 < ka_1, \tag{7}$$

$$(b_1 + k)\alpha^2 - \left(b_1^2 + ka_2\right)\alpha - b_1 b_2 < 0. \tag{8}$$

Proposition 3. *If conditions* (7) *and* (8) *are satisfied, then the equilibrium point* (x_+, z_+, u_+) *of* (3) *is locally asymptotically stable.*

To illustrate the existence of a limit cycle, this paper adopts the Hopf bifurcation theorem with α being the bifurcation parameter. It is necessary to demonstrate that the characteristic Equation (5) has a pair of purely imaginary roots along with a non-zero real root. Meanwhile, this paper aims to show that the real part of the imaginary roots exhibits non-stationary behavior when the parameter α changes. Let $\alpha = \alpha_*$ such that (7) holds true and

$$\varphi(\alpha_*) = c_1(\alpha_*)c_2(\alpha_*) - c_3(\alpha_*) = 0,$$

i.e., $(b_1 + k)\,\alpha_*^2 - \left(ka_2 + b_1^2\right)\alpha_* - b_1 b_2 = 0$. For instance, it is $\alpha_* = \left(ka_2 + b_1^2\right)/\left(b_1 + k\right)$ for $b_2 = 0, b_1 + k < 0$ and $ka_2 + b_1^2 < 0$. At the value $\alpha = \alpha_*$, $\varphi(\alpha)$ can be factored as

$$\left[\lambda + c_1(\alpha_*)\right]\left[\lambda^2 + c_2(\alpha_*)\right] = 0,$$

so the three roots are obtained $\lambda_{1,2} = \pm i\sqrt{c_2(\alpha_*)} = \pm i\omega_*$ and $\lambda_3 = -c_1(\alpha_*) < 0$. As α changes, it needs to analyze the sign of the real parts of these roots.

Differentiating Equation (5) with respect to α yields

$$\frac{d\lambda}{d\alpha} = -\frac{c_1'(\alpha)\lambda^2 + c_2'(\alpha)\lambda + c_3'(\alpha)}{3\lambda^2 + 2c_1(\alpha)\lambda + c_2(\alpha)}, \tag{9}$$

where

$$c_1'(\alpha) = 1, \qquad c_2'(\alpha) = -\left(b_1 + k\right), \qquad c_3'(\alpha) = -\left(ka_2 + b_2\right) > 0.$$

From (9), let $\lambda = i\omega_*$, and then a direct calculation produces the following result

$$\begin{aligned} Re\left(\frac{d\lambda}{d\alpha}\right)_{\alpha=\alpha_*} &= \frac{-c_1'(\alpha_*)c_2(\alpha_*) - c_1(\alpha_*)c_2'(\alpha_*) + c_3'(\alpha_*)}{2\left[c_1^2(\alpha_*) + c_2(\alpha_*)\right]} \\ &= \frac{\alpha b_1 + b_1\left(-b_1 + \alpha_*\right) - ka_2}{2\left[\left(-b_1 + \alpha_*\right)^2 - b_2 - \alpha b_1\right]}. \end{aligned}$$

Since α_* is a solution to $b_1\alpha_*^2 - \left(ka_2 + b_1^2\right)\alpha_* - b_1 b_2 = 0$, we have

$$\text{sign}\left[Re\left(\frac{d\lambda}{d\alpha}\right)_{\alpha=\alpha_*}\right] = \text{sign}\left(2b_1\alpha_* - ka_2 - b_1^2\right) = \text{sign}\left(\pm\sqrt{\left(ka_2 + b_1^2\right)^2 + 4b_1^2 b_2}\right). \tag{10}$$

A left-to-right crossing of the imaginary axis corresponds to a positive sign of (10), while a right-to-left crossing corresponds to a negative sign of (10).

Theorem 4. *The stability of the equilibrium point (x_+, z_+, u_+) may be lost and recovered at $\alpha = \alpha_*$. In both cases, Hopf bifurcations occur.*

4. Strong Kernel Case

The new variables u and v are introduced as

$$u = \int_{-\infty}^{t} z(s)\alpha^2(t-s)e^{-\alpha(t-s)}ds, \qquad v = \int_{-\infty}^{t} z(s)\alpha e^{-\alpha(t-s)}ds,$$

and system (2) can be rewritten as

$$\begin{cases} \dot{x} &= \dfrac{x(1-x)}{\varepsilon} - \dfrac{h_1 z}{\varepsilon}\dfrac{x-q}{x+q}, \\ \dot{z} &= x - z + ku, \\ \dot{u} &= \alpha\left(v - u\right), \\ \dot{v} &= \alpha\left(z - v\right). \end{cases} \tag{11}$$

In this case, the characteristic equation of the linearized system of (11) around the equilibrium point (x_+, z_+, u_+, v_+), where $u_+ = v_+ = z_+$, takes the following form

$$\begin{vmatrix} a_1 - \lambda & a_2 & 0 & 0 \\ 1 & -1-\lambda & k & 0 \\ 0 & 0 & -\alpha-\lambda & \alpha \\ 0 & \alpha & 0 & -\alpha-\lambda \end{vmatrix} = 0,$$

which leads to

$$\lambda^4 + d_1(\alpha)\lambda^3 + d_2(\alpha)\lambda^2 + d_3(\alpha)\lambda + d_4(\alpha) = 0, \tag{12}$$

where

$$\begin{aligned} d_1(\alpha) &= 2\alpha - b_1, \qquad d_2(\alpha) = \alpha^2 - 2b_1\alpha - b_2, \\ d_3(\alpha) &= \left(-b_1 - k\right)\alpha^2 - 2b_2\alpha, \qquad d_4(\alpha) = \left(ka_1 - b_2\right)\alpha^2. \end{aligned}$$

4.1. Case $d_4(\alpha) = 0$

Equation (12) reduces to

$$Q(\lambda, \alpha) = \lambda^4 + d_1(\alpha)\lambda^3 + d_2(\alpha)\lambda^2 + d_3(\alpha)\lambda = 0, \tag{13}$$

Proposition 5.

(1) *If $d_3(\alpha) \neq 0$, then $\lambda = 0$ is a simple zero root of Equation (13). The equilibrium point (x_+, z_+, u_+, v_+) of (13) is stable if and only if $d_1(\alpha) > 0, d_3(\alpha) > 0$ and $d_1(\alpha)d_2(\alpha) > d_3(\alpha)$. There exists a pair of purely imaginary roots $\pm i\omega_*$, where $\omega_* = \sqrt{d_2(\alpha_*)}$, for $\alpha = \alpha_*$ such that $d_2(\alpha) > 0$ and $-d_1(\alpha)d_2(\alpha) + d_3(\alpha) = 0$.*

(2) *If $d_3(\alpha) = 0$ and $d_2(\alpha) \neq 0$, then $\lambda = 0$ is a double root of Equation (13). The equilibrium point (x_+, z_+, u_+, v_+) of (13) is stable if and only if $d_1(\alpha) > 0$, $d_2(\alpha) > 0$. There exists a pair of purely imaginary roots $\pm i\omega_*$, where $\omega_* = \sqrt{d_2(\alpha_*)}$, for $\alpha = \alpha_*$ such that $d_2(\alpha) > 0$ and $d_1(\alpha) = 0$.*

(3) *If* $d_3(\alpha)=0$, $d_2(\alpha)=0$ *and* $d_1(\alpha)\neq 0$, *then* $\lambda=0$ *is a triple root of Equation* (13), *and the remaining root is given by* $\lambda=-d_1(\alpha)$.

(4) *If* $d_3(\alpha)=0$, $d_2(\alpha)=0$, $d_1(\alpha)=0$, *then* $\lambda=0$ *is a quadruple root of Equation* (13).

Proof. The first part of the statement is as follows

$$\frac{\partial Q(\lambda,\alpha)}{\partial\lambda}=4\lambda^3+3d_1(\alpha)\lambda^2+2d_2(\alpha)\lambda+d_3(\alpha),\qquad \frac{\partial^2 Q(\lambda,\alpha)}{\partial\lambda^2}=12\lambda^2+6d_1(\alpha)\lambda+2d_2(\alpha),$$

$$\frac{\partial^3 Q(\lambda,\alpha)}{\partial\lambda^3}=24\lambda+6d_1(\alpha),\qquad \frac{\partial^4 Q(\lambda,\alpha)}{\partial\lambda^4}=24.$$

(1) The Routh-Hurwitz criterion indicates that all roots of Equation (13) have a negative real part, except for a zero root, if and only if $d_1(\alpha)>0, d_3(\alpha)>0$ and $d_1(\alpha)d_2(\alpha)>d_3(\alpha)$. Regarding the existence of a pair of purely imaginary roots, letting $\lambda=i\omega$, where ω is real and positive, and separating (13) into real and imaginary parts, we have $-\omega^2+d_2(\alpha)=0$, $-d_1(\alpha)\omega^2+d_3(\alpha)=0$. Thus, there is $\omega=\sqrt{d_2(\alpha)}$ if $d_2(\alpha)>0$ and $-d_1(\alpha)d_2(\alpha)+d_3(\alpha)=0$.

(2) In this case, the stability of the equilibrium point is guaranteed if and only if $d_1(\alpha)>0$, $d_2(\alpha)>0$. If $\lambda=i\omega$ $(\omega>0)$ is a root of Equation (13), and then the following must hold

$$-\omega^2+d_2(\alpha)=0,\qquad d_1(\alpha)=0,$$

yielding $\omega=\sqrt{d_2(\alpha)}$ when $d_2(\alpha)>0$. The proof is complete. □

Remark 6. *Conditions* $d_1(\alpha)>0, d_3(\alpha)>0$ *and* $d_1(\alpha)d_2(\alpha)>d_3(\alpha)$ *are equivalent to*

$$\alpha>\frac{b_1}{2},\qquad (-b_1-k)\,\alpha-2b_2>0,\qquad 2\alpha^3+(k-4b_1)\,\alpha^2+2b_1^2\alpha+b_1b_2>0.$$

Proposition 7.

(1) *The equilibrium point* (x_+,z_+,u_+,v_+) *of* (13) *remains unstable if* $-\alpha_*+2\,(b_1+b_2)<0$, *and it becomes stable if* $-\alpha_*+2\,(b_1+b_2)<0$, *for* $\alpha=\alpha_*$ *such that* $d_2(\alpha)>0$ *and* $-d_1(\alpha)d_2(\alpha)+d_3(\alpha)=0$. *A Hopf bifurcation occurs at* $\alpha=\alpha_*$.

(2) *The equilibrium point* (x_+,z_+,u_+,v_+) *of* (13) *has no stability switch* (*from unstable to stable*) *at* $\alpha=\alpha_*>0$, *where* α_* *solves* $d_1(\alpha_*)=0$ *and* $d_2(\alpha_*)>0$.

Proof. (1) Taking derivative of α in (13) yields

$$\begin{aligned}
Re\left(\frac{d\lambda}{d\alpha}\right)_{\lambda=i\omega_*} &= Re\left[-\frac{d_1'(\alpha)\lambda^2+d_2'(\alpha)\lambda+d_3'(\alpha)}{3\lambda^2+2d_1(\alpha)\lambda+d_2(\alpha)}\right]_{\lambda=i\omega_*}\\
&= \frac{\left[-2d_2'(\alpha_*)\omega_*^2d_1(\alpha_*)\right]\omega_*^2-\left[d_2(\alpha_*)-3\omega_*^2\right]\left[d_3'(\alpha_*)-d_1'(\alpha_*)\omega_*^2\right]}{\left[-3\omega_*^2+d_2(\alpha_*)\right]^2+4d_1^2(\alpha_*)\omega_*^2}\\
&= \frac{\left[-\alpha_*+2\,(b_1+b_2)\right]\alpha_*}{\omega_*^2+(2\alpha-b_1)^2}
\end{aligned}$$

since

$$d_1'(\alpha_*)=2,\qquad d_2'(\alpha_*)=2\,(\alpha_*-b_1)\,,\qquad d_3'(\alpha_*)=-2\,(b_1+k)\,\alpha_*^2-2b_2,$$

and

$$\omega_*^2=d_2(\alpha_*)\qquad -2\alpha_*^3+(4b_1-k)\,\alpha_*^2-2b_1^2\alpha_*-b_1b_2=0.$$

As a result,

$$\operatorname{sign}\left[Re\left(\frac{d\lambda}{d\alpha}\right)_{\lambda=i\omega_*}\right]=\operatorname{sign}\left[-\alpha_*+2\,(b_1+b_2)\right].$$

A positive sign indicates crossing of the imaginary axis from right to left, while a negative sign denotes crossing from left to right.

(2) Differentiating (13) implicitly with respect to α and evaluating the derivatives at $\lambda = i\omega_*$, we have

$$Re\left(\frac{d\lambda}{d\alpha}\right)_{\lambda=i\omega_*} = Re\left[-\frac{d_1'(\alpha)\lambda + d_2'(\alpha)}{2\lambda + d_1(\alpha)}\right]_{\lambda=i\omega_*} = -\frac{2d_1'(\alpha_*)d_2(\alpha_*) + d_2'(\alpha_*)d_1(\alpha_*)}{4\omega_*^2 + d_1^2(\alpha_*)} = -1.$$

since $d_1'(\alpha_*) = 2$, $\omega_*^2 = d_2(\alpha_*)$ and $d_1(\alpha_*) = 0$. □

4.2. Case $d_4(\alpha) \neq 0$

According to the Routh-Hurwitz criteria for stable roots, the equilibrium point is locally asymptotically stable if and only if $d_1(\alpha) > 0, d_3(\alpha) > 0, d_4(\alpha) > 0$ and $d_1(\alpha)d_2(\alpha)d_3(\alpha) > d_3^2(\alpha) + d_1^2(\alpha)d_4(\alpha)$. Particularly, it follows $d_2(\alpha) > 0$. This leads to the following conditions

$$\alpha > \frac{b_1}{2}, \qquad (b_1 + k)\,\alpha + 2b_2 < 0, \qquad ka_1 - b_2 > 0, \tag{14}$$

$$-2\,(b_1 + k)\,\alpha^4 + \left(-k^2 + 3kb_1 - 4a_1k + 4b_1^2\right)\alpha^3 + 2\left(-kb_2 - b_1^3 + 2b_1b_2 - kb_1^2 + 2ka_1b_1\right)\alpha^2 - b_1\,(kb_2 + 4b_1b_2 + ka_1b_1)\,\alpha - 2b_1b_2^2 > 0. \tag{15}$$

Proposition 8. *If conditions* (14) *and* (15) *hold, then the equilibrium point* (x_+, z_+, u_+, v_+) *of* (11) *is locally asymptotically stable.*

Let us go back to Equation (12) to demonstrate the existence of a limit cycle. Take α as the bifurcation parameter and let $\alpha = \alpha_*$ such that (14) is verified and

$$\psi(\alpha_*) = d_1(\alpha_*)d_2(\alpha_*)d_3(\alpha_*) - d_3^2(\alpha_*) - d_1^2(\alpha_*)d_4(\alpha_*) = 0. \tag{16}$$

Note that $\psi(\alpha) = 0$ has solutions for $b_1 + k < 0$ and $b_1 > 0$ or $b_1 + k > 0$ and $b_1 < 0$. The characteristic Equation (12) can be rewritten as

$$\left[d_1(\alpha_*)\lambda^2 + d_3(\alpha_*)\right]\left[d_1(\alpha_*)\lambda^2 + d_1^2(\alpha_*)\lambda + d_1(\alpha_*)d_2(\alpha_*) - d_3(\alpha_*)\right] = 0,$$

The above equation can be solved by the following two pure imaginary roots

$$\lambda_{1,2} = \pm i\sqrt{\frac{d_3(\alpha_*)}{d_1(\alpha_*)}} = \pm i\omega_*,$$

and the roots

$$\lambda_{3,4} = \frac{-d_1^2(\alpha_*) \pm \sqrt{d_1^4(\alpha_*) - 4d_1(\alpha_*)\left[d_1(\alpha_*)d_2(\alpha_*) - d_3(\alpha_*)\right]}}{2d_1(\alpha_*)},$$

whose real parts are different from zero as

$$\lambda_3 + \lambda_4 = -d_1(\alpha_*) < 0, \qquad \lambda_3\lambda_4 = \frac{d_1(\alpha_*)d_2(\alpha_*) - d_3(\alpha_*)}{d_1(\alpha_*)} > 0.$$

Differentiating (12) with respect to α yields

$$\frac{d\lambda}{d\alpha} = -\frac{d_1'(\alpha)\lambda^3 + d_2'(\alpha)\lambda^2 + d_3'(\alpha)\lambda + d_4'(\alpha)}{4\lambda^3 + 3d_1(\alpha)\lambda^2 + 2d_2(\alpha)\lambda + d_3(\alpha)}, \tag{17}$$

where

$$d_1'(\alpha) = 2, \qquad d_2'(\alpha) = 2\,(\alpha - b_1)\,, \qquad d_3'(\alpha) = 2\left[(-b_1 - k)\,\alpha - b_2\right], \qquad d_4'(\alpha) = 2\,(ka_1 - b_2)\,\alpha.$$

Substituting $\lambda = i\omega_*$ into (17), we have

$$Re\left(\frac{d\lambda}{d\alpha}\right)_{\alpha=\alpha_*} = -\frac{d_1(\alpha_*)\psi'(\alpha_*)}{2\left\{d_1^3(\alpha_*)d_3(\alpha_*) + \left[d_1(\alpha_*)d_2(\alpha_*) - 2d_3(\alpha_*)\right]^2\right\}},$$

where

$$\psi'(\alpha_*) = d_1'(\alpha_*)d_2(\alpha_*)d_3(\alpha_*) + d_1(\alpha_*)d_2'(\alpha_*)d_3(\alpha_*) + d_1(\alpha_*)d_2(\alpha_*)d_3'(\alpha_*) - 2d_3(\alpha_*)d_3'(\alpha_*) - 2d_1(\alpha_*)d_1'(\alpha_*)d_4(\alpha_*) - d_1^2(\alpha_*)d_4'(\alpha_*).$$

Using (16) and through a series of computations, it can be deduced that

$$\operatorname{sign}\left[Re\left(\frac{d\lambda}{d\alpha}\right)_{\alpha=\alpha_*}\right] = \operatorname{sign}\left[-\psi'(\alpha_*)\right] = sign\left[\theta\left(\alpha_*\right)\right],$$

where

$$\theta\left(\alpha_*\right) = 4\left(2k + 2b_1 - b_2 + ka_1\right)\alpha_*^3 + \left(8b_2 + 4ka_1 - 9kb_1 - 12b_1^2 + 4b_1b_2 + 3k^2 - 4ka_1b_1\right)\alpha_*^2 + \left(-b_1^2b_2 + 4kb_2 + 4b_1^3 - 16b_1b_2 + 4kb_1^2 + ka_1b_1^2\right)\alpha_* + b_1\left(kb_2 + 6b_1b_2 - ka_1b_1\right).$$

A positive (resp. negative) sign indicates that increasing the value of α causes the imaginary axis to pass from right to left (resp. from left to right). The following conclusions can be obtained as a result of our analysis.

Theorem 9. *The equilibrium* (x_+, z_+, u_+, v_+) *of* (11) *may undergo stability switches when* α *crosses the values* α_* *via a Hopf bifurcation.*

5. Numerical Results

In this section, examples are provided to elucidate the theoretical results. Let $h_1 = 2/3$, $\varepsilon = 0.04$, and $q = 0.0008$. The next two examples correspond to weak and strong kernels, respectively.

Example 1. First, the following system featuring a weak kernel is investigated:

$$\begin{cases} \dot{x} &= \dfrac{x(1-x)}{25} - \dfrac{2z}{75}\dfrac{x - 0.0008}{x + 0.0008}, \\ \dot{z} &= x - z + ku, \\ \dot{u} &= \alpha(x - u). \end{cases} \tag{18}$$

In this scenario, $c_3(\alpha) > 0$ is first computed for all α and k. Then, the simulation results based on Section 3.2 can be derived. Let $k = -0.6$, it can be found that $b_1 = -34.4615$ and $b_2 = -50.1053$, with the characteristic equation of system (18) satisfying conditions (7) and (8). The equilibrium point (x_+, y_+, u_+) is proven to be locally asymptotically stable for all $\alpha > 0$. Three specific values of α, namely $\alpha = 5, 2, 0.6$, are arbitrarily chosen, and the corresponding simulation results are demonstrated in Figure 1. As the value of parameter α increases, the system exhibits greater stability.

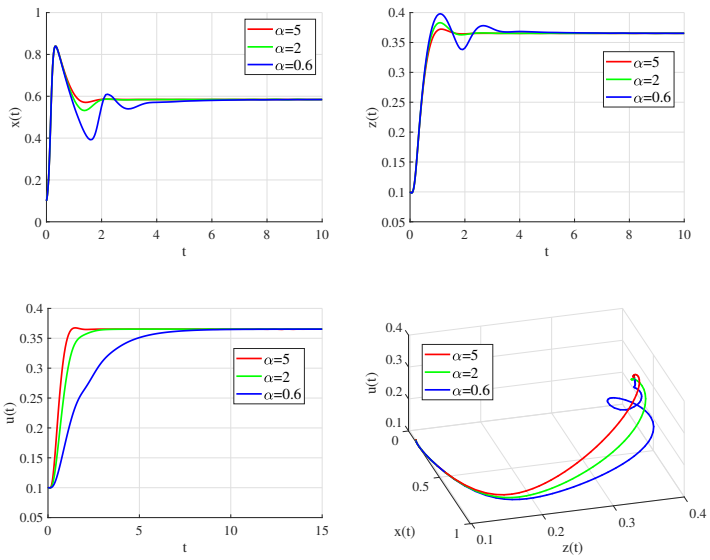

Figure 1. The waveform and phase plot of the system (18) with $k = -0.6$, which is locally asymptotically stable for $\alpha = 5,\ 2,\ 0.6$.

Next, when $k = -0.45$, the characteristic equation of system (18) will not satisfy condition (8). Then, $\alpha_* = 1.08$ is calculated, and we have $\text{sign}\left[Re\left(d\lambda/d\alpha\right)_{\alpha=\alpha_*}\right] = \text{sign}\left(2b_1\alpha_* - ka_2 - b_1^2\right) = -983.2332 < 0$. This analysis indicates that the stability of the equilibrium point (x_+, z_+, u_+) is restored as the value of α increases, and Hopf bifurcations occur as the value of α decreases. Applying Theorem 4, it is evident that the equilibrium (x_+, z_+, u_+) exhibits local asymptotic stability when $\alpha = 1.12 > \alpha_*$. It becomes unstable for $\alpha = 1.0 < \alpha_*$, and the Hopf bifurcation diverges from the equilibrium state, as demonstrated in Figures 2 and 3, respectively.

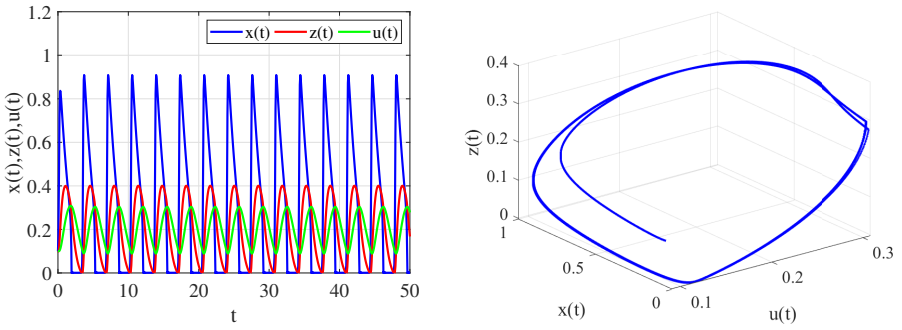

Figure 2. The waveform and phase plot of the system (18) with $k = -0.45$, and Hopf bifurcation occurs for $\alpha = 1.0 < \alpha_*$.

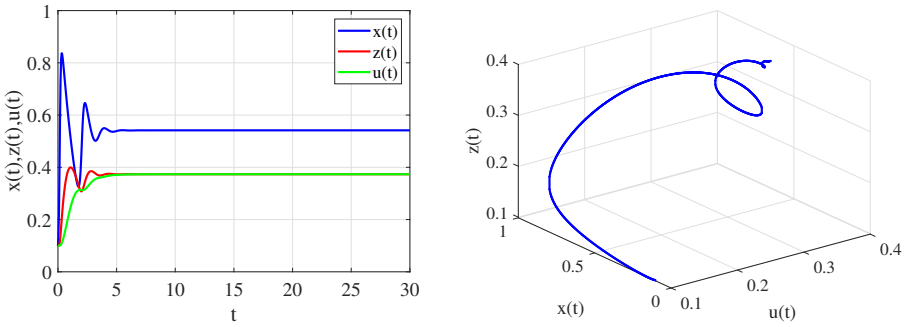

Figure 3. The waveform and phase plot of the system (18) with $k = -0.45$, which is locally asymptotically stable for $\alpha = 1.12 > \alpha_*$.

Example 2. The following system with a strong kernel is investigated:

$$\begin{cases} \dot{x} &= \dfrac{x(1-x)}{25} - \dfrac{2z}{75}\dfrac{x-0.0008}{x+0.0008}, \\ \dot{z} &= x - z + ku, \\ \dot{u} &= \alpha\left(v-u\right), \\ \dot{v} &= \alpha\left(z-v\right). \end{cases} \tag{19}$$

Similarly to the previous example, $k = -0.6$ is set, and $d_4(\alpha) > 0$ is calculated. Then, it is found that the characteristic equation of system (19) satisfies conditions (14) and (15). In this case, the equilibrium point (x_+, y_+, u_+, v_+) is locally asymptotically stable for all $\alpha > 0$, as depicted in Figure 4.

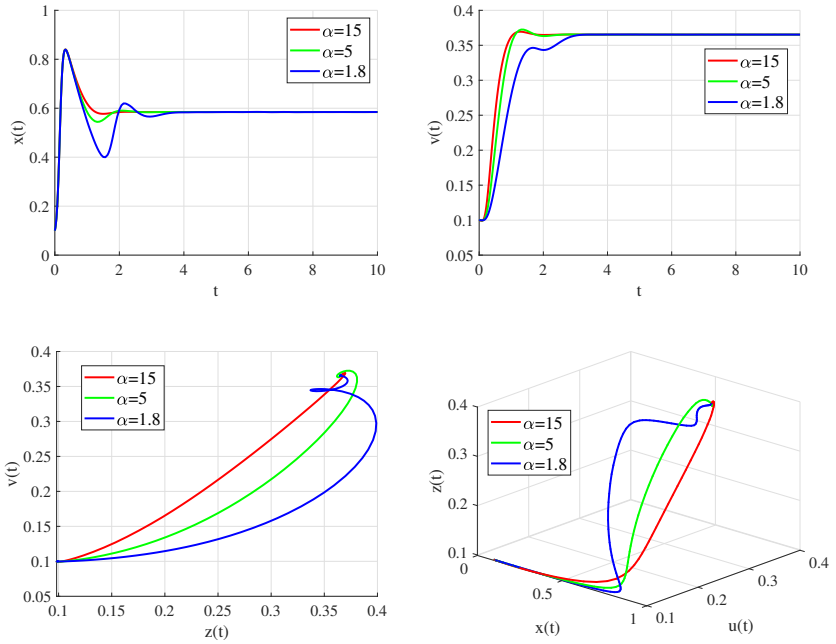

Figure 4. The waveform and phase plot of the system (19) with $k = -0.6$, which is locally asymptotically stable for $\alpha = 15, 5, 1.8$.

Next, when $k = -0.45$, the characteristic equation of the system (19) does not satisfy the condition (15). $\alpha_* = 2.62$ is computed, and it is found that $\theta(\alpha_*) < 0$. Utilizing Theorem 9, for $\alpha = 2.8 > \alpha_*$, the equilibrium (x_+, z_+, u_+, v_+) shows local asymptotic stability at α_*. Meanwhile, when $\alpha = 2.4 < \alpha_*$, it becomes unstable, and the Hopf bifurcation deviates from the equilibrium state, as demonstrated in Figures 5 and 6 respectively.

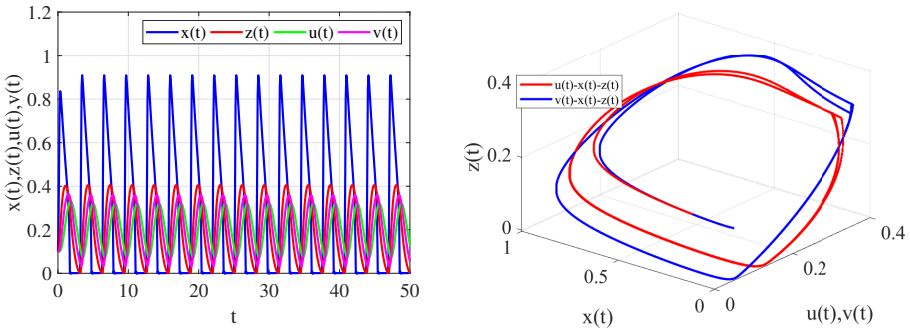

Figure 5. The waveform and phase plot of the system (19) with $k = -0.45$, and Hopf bifurcation occurs for $\alpha = 2.4 < \alpha_*$.

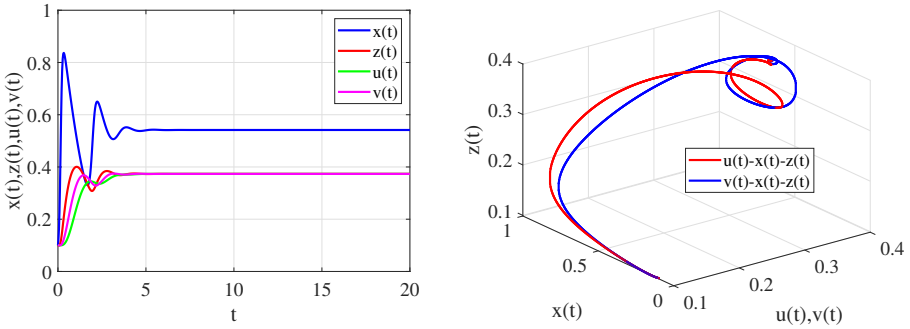

Figure 6. The waveform and phase plot of the system (19) with $k = -0.45$, which is locally asymptotically stable for $\alpha = 2.6 > \alpha_*$.

6. Conclusions

This paper thoroughly studies the bifurcation problem of the Oregonator oscillator with a distributed time delay. By considering the cases of weak and strong kernels, the stability and Hopf bifurcation within the Oregonator oscillator system with distributed delays is discussed. Meanwhile, the Routh-Hurwitz criterion is employed, which lays a solid theoretical foundation for investigating these aspects. Finally, the efficacy of our approach is validated through simulation examples. The results suggest that under identical parameter settings, compared to the case with a weak kernel, the unstable region in the case with a strong kernel is more extensive. The derived criteria and results not only improve our understanding of the system's behavior but also provide practical guidelines for bifurcation prediction and control in future studies.

Author Contributions: Y.W.: software, visualization, validation, writing—original draft preparation, writing—reviewing and editing; L.G.: conceptualization, methodology, writing—original draft preparation, writing—reviewing and editing. All authors have read and agreed to the published version of the manuscript.

Funding: This research received no external funding.

Institutional Review Board Statement: Not applicable.

Informed Consent Statement: Not applicable.

Data Availability Statement: Not applicable.

Conflicts of Interest: The authors declare no conflict of interest.

References

1. Zhao, H.; Wang, L. Hopf bifurcation in Cohen–Grossberg neural network with distributed delays. *Nonlinear Anal. Real World Appl.* **2007**, *8*, 73–89.
2. Song, Y.; Yuan, S. Bifurcation analysis in a predator–prey system with time delay. *Nonlinear Anal. Real World Appl.* **2006**, *7*, 265–284.
3. Xu, W.; Cao, J.; Xiao, M.; Ho, D.W.; Wen, G. A new framework for analysis on stability and bifurcation in a class of neural networks with discrete and distributed delays. *IEEE Trans. Cybern.* **2014**, *45*, 2224–2236.
4. Li, L.; Wang, Z.; Li, Y.; Shen, H.; Lu, J. Hopf bifurcation analysis of a complex-valued neural network model with discrete and distributed delays. *Appl. Math. Comput.* **2018**, *330*, 152–169.
5. Cao, Y. Bifurcations in an Internet congestion control system with distributed delay. *Appl. Math. Comput.* **2019**, *347*, 54–63.
6. Shukla, A.; Patel, R. Controllability results for fractional semilinear delay control systems. *J. Appl. Math. Comput.* **2021**, *65*, 861–875.
7. Sardar, M.; Biswas, S.; Khajanchi, S. The impact of distributed time delay in a tumor-immune interaction system. *Chaos, Solitons Fractals* **2021**, *142*, 110483.
8. Beretta, E.; Hara, T.; Ma, W.; Takeuchi, Y. Global asymptotic stability of an SIR epidemic model with distributed time delay. *Nonlinear Anal. Theory Methods Appl.***2001**, *47*, 4107–4115.
9. Ibrahim, L.M. Anomaly network intrusion detection system based on distributed time-delay neural network (DTDNN). *J. Eng. Sci. Technol.***2010**, *5*, 457–471.
10. Zhang, H.; Cheng, Y.; Zhang, W.; Zhang, H. Time-dependent and Caputo derivative order-dependent quasi-uniform synchronization on fuzzy neural networks with proportional and distributed delays. *Math. Comput. Simul.***2023**, *203*, 846–857.
11. Bray, W.C. A periodic reaction in homogeneous solution and its relation to catalysis. *Math. Comput. Simul.***1921**, *43*, 1262–1267.
12. Zhabotinsky, A.M. Periodic oxidizing reactions in the liquid phase. In *Doklady Akademii Nauk*; Russian Academy of Sciences: Moscow, Russia. **1964**, *157*, 392–395.
13. Sriram, K.; Bernard, S. Complex dynamics in the Oregonator model with linear delayed feedback. *Chaos* **2008**, *18*, 023126.
14. Wu, X.; Zhang, C. Dynamic properties of the Oregonator model with delay. *J. Appl. Anal. Comput.* **2012**, *2*, 91–102.
15. Liu, Z.; Yuan, R. Zero-Hopf bifurcation for an infection-age structured epidemic model with a nonlinear incidence rate. *Sci. China Math.* **2017**, *60*, 1371–1398.
16. Cai, Y.; Liu, L.; Zhang, C. Hopf-zero bifurcation of Oregonator oscillator with delay. *Adv. Differ. Equ.* **2018**, *2018*, 438.

17. Xu, C.; Aouiti, C.; Liu, Z.; Li, P.; Yao, L. Bifurcation caused by delay in a fractional-order coupled oregonator model in chemistry. *Match Commun. Math. Comput. Chem.* **2022**, *88*, 371–396.
18. Song, Y.; Jiang, J. Steady-state, Hopf and steady-state-Hopf bifurcations in delay differential equations with applications to a damped harmonic oscillator with delay feedback. *Int. J. Bifurcation Chaos* **2012**, *22*, 1250286.
19. Su, R.; Zhang, C. Hopf-zero bifurcation of the ring unidirectionally coupled Toda oscillators with delay. *Nonlinear Anal. Model. Control* **2021**, *26*, 375–395.
20. Xu, C.; Zhang, W.; Aouiti, C.; Liu, Z.X.; Li, P.L.; Yao, L. Bifurcation dynamics in a fractional-order Oregonator model including time delay. *MATCH Commun. Math. Comput. Chem.* **2022**, *87*, 397–414.
21. Gao, S.; Teng, Z.; Nieto, J.J.; Torres, A. Analysis of an SIR epidemic model with pulse vaccination and distributed time delay. *Biomed Res. Int.* **2007**, *1*, 064870.
22. Adimy, M.; Crauste, F.; Ruan, S. Stability and Hopf bifurcation in a mathematical model of pluripotent stem cell dynamics. *Nonlinear Anal. Real World Appl.* **2005**, *6*, 651–670.
23. Zhao, H.; Lin, Y.; Dai, Y. Hopf bifurcation and hidden attractors of a delay-coupled Duffing oscillator. *Int. J. Bifurcation Chaos* **2015**, *25*, 1550162.
24. Xu, S.; Bao, J. Distributed control of plant-wide chemical processes with uncertain time-delays. *Chem. Eng. Sci.* **2012**, *84*, 512–532.
25. Dvorak, A.; Kuzma, P.; Perlikowski, P.; Astakhov, V.; Kapitaniak, T. Dynamics of three Toda oscillators with nonlinear unidirectional coupling. *Eur. Phys. J. Spec. Top.* **2013**, *222*, 2429–2439.
26. Lipták, G.; Pituk, M.; Hangos, K.M. Modelling and stability analysis of complex balanced kinetic systems with distributed time delays. *J. Process Control* **2019**, *84*, 13–23.
27. Komatsu, H.; Nakajima, H. Stability analysis for single linkage class chemical reaction networks with distributed time delays. *IFAC-PapersOnLine* **2023**, *56*, 10466–10471.
28. Rihan, F.A.; Alsakaji, H.J.; Rajivganthi, C. Stochastic SIRC epidemic model with time-delay for COVID-19. *Adv. Differ. Equ.* **2020**, *2020*, 502.
29. Polifke, W. Modeling and analysis of premixed flame dynamics by means of distributed time delays. *Prog. Energy Combust. Sci.* **2020**, *79*, 100845.
30. MacDonald, N. *Time Lags in Biological Models*; Springer Science & Business Media: Berlin, Germany, 2013.
31. Cushing, J.M. *Integrodifferential Equations and Delay Models in Population Dynamics*; Springer Science & Business Media: Berlin, Germany, 2013.